JAAS

Accepted Manuscript

This is an *Accepted Manuscript*, which has been through the Royal Society of Chemistry peer review process and has been accepted for publication.

Accepted Manuscripts are published online shortly after acceptance, before technical editing, formatting and proof reading. Using this free service, authors can make their results available to the community, in citable form, before we publish the edited article. We will replace this *Accepted Manuscript* with the edited and formatted *Advance Article* as soon as it is available.

You can find more information about *Accepted Manuscripts* in the Information for Authors.

Please note that technical editing may introduce minor changes to the text and/or graphics, which may alter content. The journal's standard Terms & Conditions and the Ethical guidelines still apply. In no event shall the Royal Society of Chemistry be held responsible for any errors or omissions in this *Accepted Manuscript* or any consequences arising from the use of any information it contains.

ROYAL SOCIETY OF CHEMISTRY

www.rsc.org/jaas

Journal Name

ARTICLE

Magnetic field enhancement for femtosecond-laser-ablation mass spectrometry in ambient environments

Received 00th January 20xx,
Accepted 00th January 20xx

DOI: 10.1039/x0xx00000x

www.rsc.org/

Y. Lu,[a] Y. S. Zhou,[a,*] W. Qiu,[b] X. Huang,[a] L. Liu,[a] L. Jiang,[c] J. F. Silvain,[a,d] and Y. F. Lu[a,*]

To improve the sensitivity of open-air femtosecond-laser-ablation mass spectrometry (fs-LA-MS), an external magnetic field was introduced to confine the propagation of the plasma, reduce the plasma neutralization rates, and drive charged particles towards the MS orifice. Signal-to-noise ratios (SNRs) of trace elements, including Al, Si and Pb, in standard NIST samples were obviously improved. The SNR enhancement depends strongly on the direction of the magnetic fields. The maximum enhancement factors were obtained when directing the magnetic fields towards the orifice of the mass spectrometer. The enhancement factors (EFs) of 8.30, 8.22 and 8.50 were achieved for ^{206}Pb, ^{207}Pb and ^{208}Pb in pure lead. The limit of detections (LODs) of ^{206}Pb, ^{207}Pb and ^{208}Pb were lowered from 9.75, 32.9 and 8.19 ppm to 2.32, 6.02 and 1.98 ppm, respectively.

1. Introduction

Wet-chemistry methods are generally used for processing hard solid materials, such as metals and rocks, before mass spectrometric studies, and inevitably introduce undesired pollutants into the samples. Laser ablation makes it feasible for studying hard solids without sample pre-treatments,[1,2] especially for hazardous and toxic materials.[3] Laser ablation has been extensively adopted in mass spectrometry, such as laser ablation inductively coupled plasma mass spectrometry (LA-ICP-MS)[4] and laser ionization mass spectrometry (LIMS).[5-11] Both techniques have achieved LODs below ppm in a controlled environment or a vacuum chamber.[3] So far, only limited studies were reported on open-air LA-MS for studying hard solid materials. He et al.[3] reported ambient air LA-MS elemental analyses by combining laser ablation with an ambient mass spectrometer without sample pre-treatments and buffer gases. However, due to the low ionization rate in the nanosecond-laser-induced plasma and low sample collection efficiency of the ambient MS, the sensitivity of the ambient LA-MS is relatively low, which limits its extensive applications, especially in studying solid materials.

To address the challenges and improve the sensitivity of the open-air LA-MS, we combined femtosecond (fs) laser and magnetic field to increase plasma ionization rates, confine plasma propagation, and direct the movement of ions. Due to its unique strength in effective material ionization and precise ion species ratios, fs-laser ablation is suggested to be more suitable than ns-laser ablation in ionizing solid samples for elemental analysis.[12,13] In addition, an external magnetic field has been demonstrated to be effective in confining plasma propagation and directing the movement of charged particles, leading to increased plasma ionization ratios[14, 15] and collection efficiency of the MS.[16, 17] Based on the phenomena above, the sensitivity enhancement of the open-air fs-LA-MS was investigated by configuring the external magnetic fields with respect to the direction of the MS orifice. Sensitivity improvements of trace amount of Al, Si in NIST 1762 sample, and Pb in NIST 494 sample were investigated using the magnetic-field-enhanced open-air fs-LA-MS.

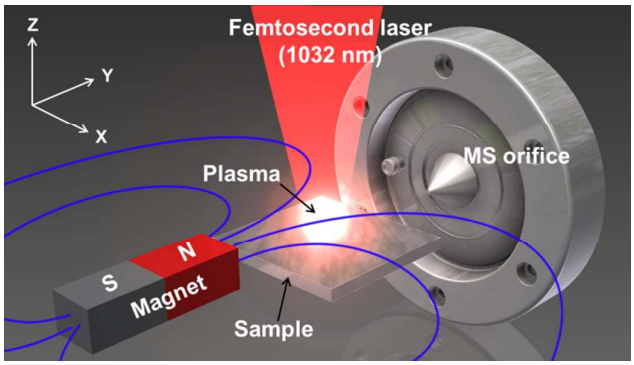

Fig. 1. Experimental setup of magnetic-field-enhanced open-air fs-LA-MS.

2. Experimental

The experimental setup used in this study is shown in Fig. 1. A near infrared (NIR) femtosecond (fs) laser (PolarOnyx Laser, Inc., Uranus 3200-1030-0800-PM, central wavelength of 1032 nm, pulse duration of 600 fs, pulse energy of 150 μJ, and repetition rate of

[a] Department of Electrical and Computer Engineering, University of Nebraska-Lincoln, Lincoln, NE 68588-0511，United States
[b] Department of Mechanics, Tianjin University, Tianjin, 300072, PR China
[c] School of Mechanical Engineering, Beijing Institute of Technology, 100081, PR China
[d] Institut de Chimie de la Matière Condensée de Bordeaux – ICMCB-CNRS 87, Avenue du Docteur Albert Schweitzer F-33608 Pessac Cedex – France
* ylu2@unl.edu yzhou5@unl.edu

150 KHz) was used as the irradiation source. The laser beam was focused onto a target at an incident angle of 90°. A sample target was placed in open air without any pre-treatment. A time-of-flight mass spectrometer (TOF-MS) (AccuTOF^{TM}, JEOL USA, Inc.) was used as the analyzer. All mass spectra were acquired in the positive ion mode. The voltages of the outer and inner orifices were set to be 30 and 5 V, respectively. The temperature of the skimmer cone was fixed at 100 °C. The acquisition range was 10-600 m/z with an acquisition time of 1 min. Every experiment was repeated 5 times.

A permanent magnet with a size of 3×1×1 in.^{3} was used to create magnetic fields. The magnet was fixed with the center axle direct to the plume generated from the sample by the fs laser as shown in Fig. 1. A Gaussian meter (Model 5080, Bell technologies Inc.) was used for measuring magnetic fields. Pure lead and standard NIST samples (494, 495, 498, 500, and 1762) were studied. Table 1 shows the concentrations of Al, Si, and Pb in corresponding NIST samples.

Table 1. Concentrations (ppm) of the trace elements, Al, Si and Pb, in the NIST samples.

NIST #	1762	494	495	498	500
Al	706	–	–	–	–
Si	3510	–	–	–	–
Pb	–	26.5	3.25	10	128

3. Results and discussion

3.1. Magnetic-field-enhanced MS signal intensity

Mass spectra of NIST 1762 and 494 samples were measured with and without the presence of an external magnetic field, respectively. Figure 2 shows the mass spectra of trace-amount of Al, Si, and Pb in NIST 1762 and 494 samples, respectively, with and without an external magnetic field (central magnitude ~ 0.25 T). The magnetic field is set to be along the Y axis as shown in Fig. 1. The samples were ablated by fs laser pulses with a peak power of 1.3 × 10^{13} W/cm^2. Table 2 lists the average signal-to-noise ratios (SNRs) of the measured elements with and without the magnetic field. As shown in Table 2, the average SNRs of Al, Si, ^{206}PbOH, ^{207}PbOH, and ^{208}PbOH in NIST 1762 and 494 samples without the presence of the magnetic field are 35.48, 7.97, 3.88, 2.25, and 4.02, respectively. Under the assistance of the external magnetic field, the corresponding SNRs are obviously increased to be 238.65, 41.14, 12.44, 4.79, and 15.05, respectively. As shown in Fig. 2, it is obvious that without the presence of the magnetic field, the Si and ^{207}PbOH signals are barely discernible compared to the background noise. However, with assistance of the magnetic field, both are clearly identified in the MS spectrum. The enhancement factors (EFs) were calculated using the SNRs of the trace elements with the presence of the magnetic field divided by the SNRs without the presence of the magnetic field. The enhancement factors for Al, Si, ^{206}PbOH, ^{207}PbOH, and ^{208}PbOH are 6.73, 5.16, 3.21, 2.13, and 3.74, respectively. The difference of the enhancement factor is ascribed to the velocities and different atomic weights of the charged particles.[18,19] For ^{206}PbOH, ^{207}PbOH, and ^{208}PbOH, they have very similar atomic weights and laser-ablation-induced velocities. The enhancement factors are in accord with their abundances in the sample.

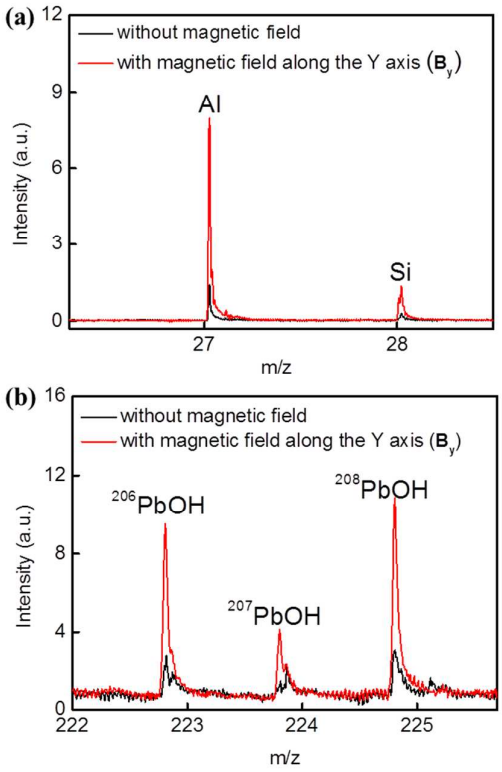

Fig. 2. MS spectra of Al, Si, ^{206}PbOH, ^{207}PbOH, and ^{208}PbOH in NIST 1762 (a) and 494 (b) samples measured using the open-air fs-LA-MS with and without the external magnetic fields (0.25 T).

Table 2. EFs of Al (NIST 1762), Si (NIST 1762), and Pb isotopes (NIST 494) under the influence of the magnetic field.

Peaks		Al	Si	^{206}PbOH	^{207}PbOH	^{208}PbOH
SNR	Without B	35.48 ± 9.05	7.97 ±1.00	3.88 ±0.69	2.25 ±0.53	4.02 ±0.52
	With B	238.65 ±23.39	41.14 ±3.70	12.44 ±1.46	4.79 ± 0.83	15.05 ±1.23
EF		6.73	5.16	3.21	2.13	3.74

3.2. Direction effect of the magnetic field

The MS enhancement factors are dependent on the direction of the magnetic field with respect to the MS orifice. In this study, the magnet was placed along the X (B_x) and Y (B_y) axes, separately. Both B_x and B_y were fixed at 0.25 T (central magnitude). The magnet and plasma center were tuned to be coaxial. Figure 3 shows the mass spectra of the pure lead with the magnetic fields along the Y axis (blue line), X axis (red line), and without magnetic fields (black line), respectively. It is observed that almost all signal intensities of Pb and PbOH, including corresponding isotopes, are enhanced with the presence of the magnetic fields (both along the X and Y axes). Table 3 lists the enhancement factors of major signals shown in Fig. 3. As

shown in Table 3, the enhancement factors of signals obtained with B_y are several times larger than those with B_x. The enhancement factors of element Pb isotopes are much higher than those of PbOH.

The enhancement factors of different Pb isotope compounds (^{206}PbOH, ^{207}PbOH, ^{208}PbOH) in pure lead are similar (Table 3), which are different from the results obtained from NIST 494 sample (Table 2). The measured PbOH signal is formed by laser ablated Pb reacting with O_2 and H_2O in open air. In NIST 494 sample (Table 2), concentrations of Pb isotopes (ppm levels) are much lower than the concentrations of O_2 (21%) and H_2O (1% to 0.4%). Therefore, the reaction rates are decided by the corresponding Pb isotope abundances. However, in pure lead sample (Table 3), H_2O in open air is much less than required to achieve complete reactions with Pb. Therefore, the reaction rates are decided by the concentration of H_2O in open air which is a constant.

3.3. Mechanisms of the magnetic-field-enhanced open-air fs-LA-MS

The MS signal enhancement shown in Figs. 2 and 3 is ascribed to the Lorenz force exerted on charged particles when moving in an inhomogeneous magnetic field, which results in the following three phenomena. The first is reduced plasma propagation rates which result in increased plasma density and prolonged plasma duration time for MS sampling. The second is increased plasma ionization rates due to increased number of collisions within a certain unit of time. The third is enhanced drifting of charged particles towards a weaker field when moving in a magnetic field gradient.

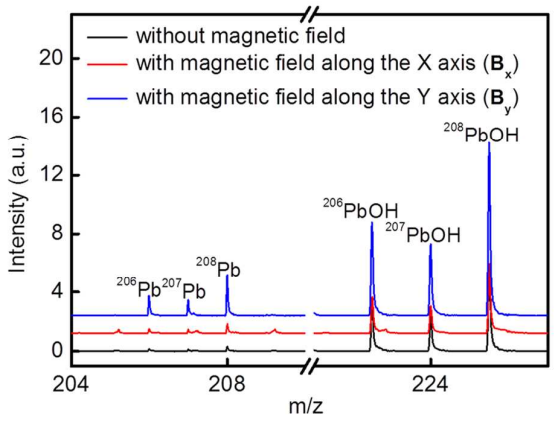

Fig. 3. The influence of magnetic field direction on the open-air fs-LA-MS analysis of pure lead sample: no magnetic field (black line), magnetic field along the X axis (red line), magnetic field along the Y axis (blue line).

Table 3. EFs of Pb and PbOH from a pure lead sample with a magnetic field along X and Y axes, respectively.

Peaks	^{206}Pb	^{207}Pb	^{208}Pb	^{206}PbOH	^{207}PbOH	^{208}PbOH
B_x	1.71	1.71	1.72	0.80	0.79	0.81
B_y	8.30	8.22	8.50	2.15	2.13	2.02

When the magnet was placed along the Y axis, the propagation of the plasma along the X and Z axes are both suppressed by the Lorenz force ($\vec{F} = \vec{v} \times \vec{B}$ for cations, and $\vec{F} = -\vec{v} \times \vec{B}$ for anions). The confinement of the plasma propagation induced by the magnetic field leads to an increased plasma density and a prolonged plasma life time.[14,20-22] With the increased plasma density, MS can sample more charged particles at a certain unit of time. Similarly, the prolonged plasma life time also increases the amount of charged particles sampled by MS. Besides, the increased plasma density increases numbers of collisions and results in the increased ionization rates within the plasma.[21,22] When the magnetic field was placed along the X axis, the propagation of the plasma along the Y and Z axes are suppressed. This configuration plays the same role in increasing the plasma density and prolonging the plasma life time with the magnet placed along the Y axis. However, the propagation along the Y axis, which is the direction towards the MS orifice, is suppressed. This is the reason why the enhancement factors with the presence of B_x are lower than those with the presence of B_y as shown both in Fig. 3 and Table 3.

The third effect comes from the inhomogeneous magnetic fields. When a charged particle moves through a magnetic gradient, it tends to drift towards a location with a weak field.[17] By appropriately placing the magnetic field gradient and pointing the weak field towards the MS orifice, the charged particles move towards the MS orifice and increase collection efficiency of the MS.

3.4. Limit of detection (LODs)

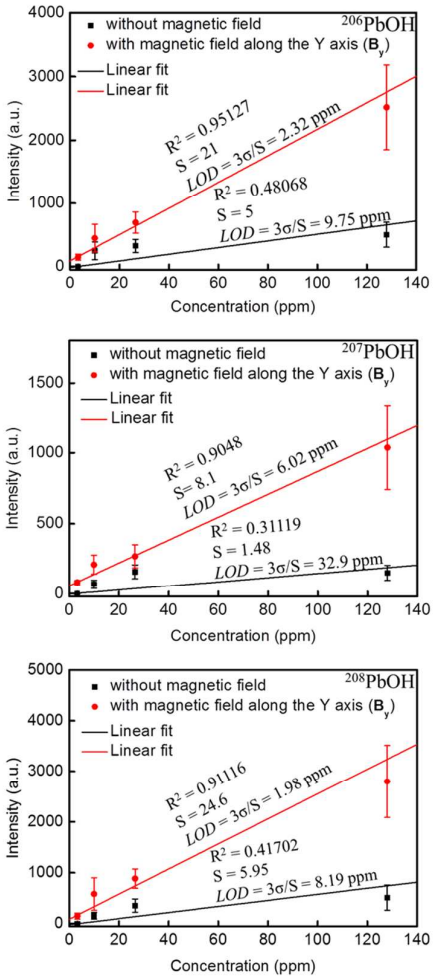

Fig. 4. Calibration curves of lead isotopes (a) ^{206}PbOH, (b) ^{207}PbOH, and (c) ^{208}PbOH in the standard NIST samples with magnetic field (red line) and without magnetic field (black line).

To investigate the limits of detection (LODs) in the magnetic-field-assisted open-air fs-LA-MS, calibration curves of lead isotope compounds with the magnetic field along the Y axis were plotted as shown in Fig. 4. NIST 494, 495, 498, and 500 samples were used as standard samples with the concentrations of lead listed in Table 1. Linear fits were performed using ORIGIN 8.5 with lead concentration and MS signal intensity without magnetic field and with magnetic field along the Y axis, respectively. According to the International Union of Pure and Applied Chemistry (IUPAC) criteria,[23] the LOD is defined as,

$$LOD = 3\sigma/S,$$

where σ is the standard deviation of the background, and S is the slope of the calibration curve. As shown in Fig. 4, the LODs of lead without the magnetic field are 9.75, 32.9, and 8.19 ppm for ^{206}PbOH, ^{207}PbOH, and ^{208}PbOH, respectively. With the presence of the magnetic field, the LODs of lead were improved for all isotope compounds which reached 2.32, 6.02, and 1.98 ppm for ^{206}PbOH, ^{207}PbOH, and ^{208}PbOH, respectively. The improvement factors (LOD without magnetic field divided by that with the magnetic field along the Y axis) are 4.2, 5.5 and 4.1 for ^{206}PbOH, ^{207}PbOH, and ^{208}PbOH, respectively.

4. Conclusion

Magnetic-field-enhanced open-air fs-LA-MS has been developed. Both signal strength and LODs of solid materials are improved by deploying external magnetic fields in the open-air fs-LA-MS. Guided by the Lorentz force, the improved sensitivity is ascribed to the reduced plasma propagation, prolonged plasma life time for MS sampling, increased plasma ionization rates, and enhanced drift of charged particle towards a weaker field when moving in a magnetic field gradient. The magnetic-field assistance enables the open-air fs-LA-MS a viable technique for studying hard solids without sample pre-treatments.

Acknowledgement

This work was financially supported by the Defense Threat Reduction Agency (through HDTRA1-12-1-0019 and HDTRA1-13-1-0019). The authors would like to thank Carl Endrulat for proofreading and grammar checking of the manuscript.

Notes and references

1 D. A. Rusak, B. C. Castle, B. W. Smith, J. D. Winefordner, Trends Anal. Chem., 1998, **17**, 453-461.
2 N. Omenetto, J. Anal. At. Spectrom., 1998, 13, 385-399.
3 X. N. He, Spectrochimica Acta Part B, 2012, **67**, 64-73.
4 R. E. Russo, X. L. Mao, H. C. Liu, J. Gonzalez, S. S. Mao, Talanta, 2002, **57**, 425-451.
5 A. Vertes, R. Gijbels, F. Adams, Laser Ionization Mass Analysis, Wiley Interscience, 1993.
6 J. He, W. Zhong, C. Mahan, W. Hang, Spectrochim. Acta Part B, 2006, **61**, 220-224.
7 W. Hang, J. Anal. At. Spectrom., 2005, **20**, 301-307.
8 D. Peng, J. He, Q. Yu, L. Chen, W. Hang, B. Huang, Spectrochim. Acta Part B, 2008, **63**, 868-874.
9 A. A. Sysoev, A. A. Sysoev, Eur. J. Mass Spectrom., 2002, **8**, 213-232.
10 J. S. Becker, H. J. Dietze, Fresenius J. Anal. Chem., 1992, **344**, 69-86.
11 J. He, R. Huang, Q. Yu, Y. Lin, W. Hang, B. Huang, J. Mass Spectrom., 2009, **44**, 780-785.
12 T. Kato, T. Kobayashi, Y, Hayashizaki, et al., Journal of Physics: Conference Series, 2007, **59**, 372-375.
13 V. Margetic, A. Pakulev, A. Stockhaus, M. Bolshov, K. Niemax, et al., Spectrochimica Acta Part B, 2000, **55**, 1771-1785.
14 I. Saxena, S. Wolff, and J. Cao, Manufacturing Letters, 2015, **3**, 1-4.
15 D. M. Hoffman, B. Singh, and J. H. Thomas, Handbook of vacuum science and technology, Elsevier Inc, 1998.
16 K. A. Pathak and A. J. Chandy, J. Appl. Phys., 2009, **105**, 084909.
17 E. H. Holt and R. E. Haskell, Foundations of plasma dynamics, Macmillan, 1965.
18 H. J. Dang, Y. X. Tang, and Q. Z. Qin, Applied Surface Science, 1998, **136**, 206-212.
19 L. V. Zhigilei and B. J. Garrison, Appl. Phys. Lett., 1997, **71**, 551-553.
20 X. K. Shen, Y.F. Lu, T. Gebre, H. Ling, and Y. X. Han, J. Appl. Phys., 2006, **100**, 053303.
21 W. Wang, J. Foster, A. E. Wndt, J. H. Booske, T. Onuoha, P. W. Sandstrom, H. Liu, S. S. Gearhart, and N. Hershkowitz, Appl. Phys. Lett., 1997, **71**, 1622-1624.
22 K. G. Kostov and J. J. Barroso, IEEE Transactions on plasma science, 2006, **34**, 1127-1135.
23 X. K. Shen, H. Wang, Z. Q. Xie, Y. Gao, H. Ling, Y. F. Lu, Appl. Opt., 2009, **48**, 2551-2558.

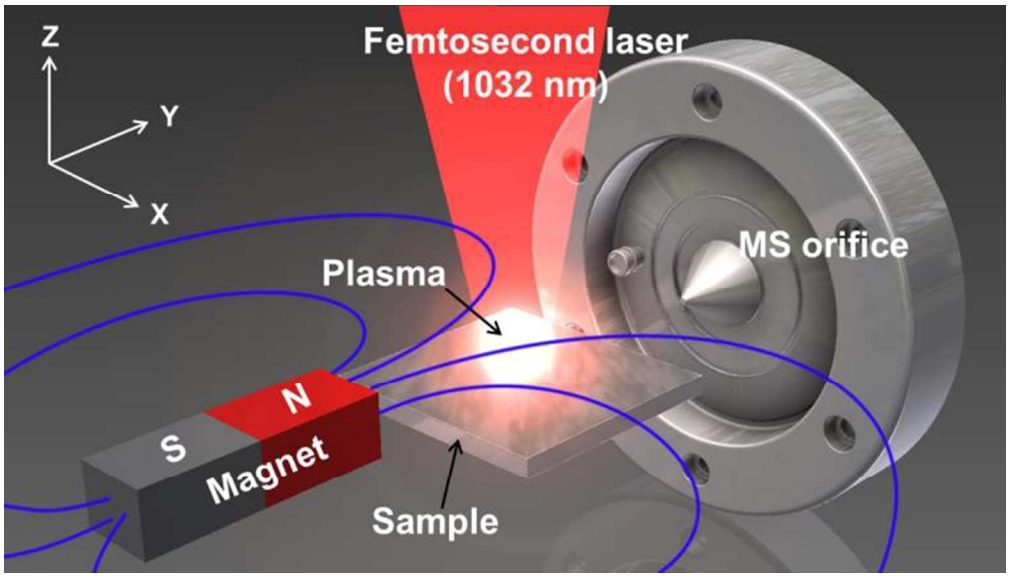

87x49mm (220 x 220 DPI)